MITSUBISHI ELECTRIC RESEARCH LABORATORIES
http://www.merl.com

An Oscillator-based Path Planning for Pocket Milling

Kalmar-Nagy, T.; Erdim, H.

TR2014-115 May 2014

Abstract

One of the most common problems in CAD/CAM is to find an optimal tool path for milling a pocket (defined by a planar shape on the x-y plane). Traditional approaches employ zigzag or contour-parallel paths. Unfortunately, these approaches typically provide paths with high curvature segments. Motions along such paths increase forces on the tool leading to increased wear and a consequent decrease in tool life. Another objective for tool path planning is to minimize the machining time. Thus for a given pocket shape we want to find the tool path such that this exact shape is machined and the tool path is good with respect to some metric. This optimization problem is very hard, so we restrict the class of admissible paths to spiral curves that wind around the initial engagement point and eventually ”track” the boundary of the pocket. Our idea is to find a function f(x,y) that is positive over the given pocket shape S and consider this function as a kind of ”energy” of a one-degree-of-freedom oscillator. We make the correspondence between the position x and velocity x of the oscillator and the spatial coordinates(x,y). If the oscillator is conservative, the trajectories are (in general) closed curves corresponding to constant energy and are level sets of f(x,x). One way to make a transition between these curves is to introduce negative damping into the equation of motion of the oscillator. A fast milling simulator based on composite adaptively sampled distance fields is discussed. We describe an algorithm that couples the oscillator-based path planner and this milling simulator to evaluate paths.

International Symposium on Tools & Methods of Competitive Engineering (TMCE)

Proceedings of TMCE 2014, May 19-23, 2014, Budapest, Hungary, Edited by I. Horváth, Z. Rusák

AN OSCILLATOR-BASED PATH PLANNING FOR POCKET MILLING

Tamas Kalmar-Nagy
Mitsubishi Electric Research Laboratories
kalmar-nagy@merl.com

Huseyin Erdim
Product Development Innovation Center, The Boeing Company
huseyin.erdim@boeing.com

Abstract

One of the most common problems in CAD/CAM is to find an optimal tool path for milling a pocket (defined by a planar shape on the x-y plane). Traditional approaches employ zigzag or contour-parallel paths. Unfortunately, these approaches typically provide paths with high curvature segments. Motions along such paths increase forces on the tool leading to increased wear and a consequent decrease in tool life. Another objective for tool path planning is to minimize the machining time. Thus for a given pocket shape we want to find the tool path such that this exact shape is machined and the tool path is good with respect to some metric. This optimization problem is very hard, so we restrict the class of admissible paths to spiral curves that wind around the initial engagement point and eventually "track" the boundary of the pocket. Our idea is to find a function f(x,y) that is positive over the given pocket shape S and consider this function as a kind of "energy" of a one-degree-of-freedom oscillator. We make the correspondence between the position x and velocity $\dot{x}$ of the oscillator and the spatial coordinates(x,y). If the oscillator is conservative, the trajectories are (in general) closed curves corresponding to constant energy and are level sets of f(x,$\dot{x}$). One way to make a transition between these curves is to introduce negative damping into the equation of motion of the oscillator. A fast milling simulator based on composite adaptively sampled distance fields is discussed. We describe an algorithm that couples the oscillator-based path planner and this milling simulator to evaluate paths.

Keywords: Pocket milling; Path planning;

1. Introduction

One of the most common problems in material removal processes is to find a good/optimal tool path for milling a pocket. In the so-called pocket milling (shown in Figure 1), the material is removed from the workpiece layer by layer. Traditional approaches employ zigzag or contour-parallel paths (Figures 2a and 2b).

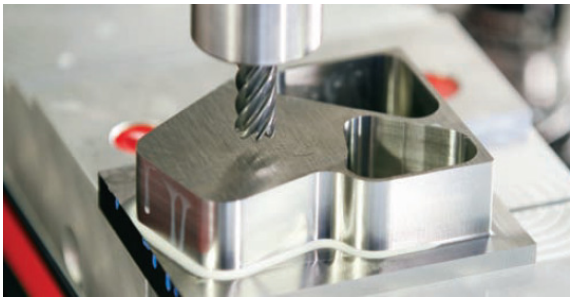

Figure 1. Pocket milling

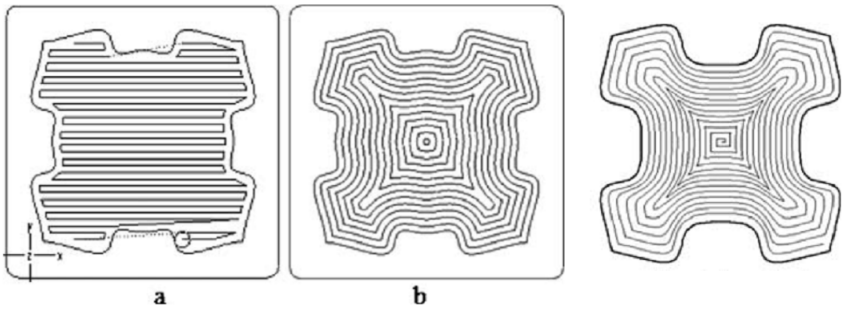

Figure 2. Pocket milling strategies: (a) zigzag machining (b) contour-parallel machining (c) spiral contouring

Unfortunately, these paths typically have high curvature segments. Motions along such paths increase forces on the tool, leading to increased wear and a consequent decrease in tool life. In addition to avoiding harmful cutting conditions, another objective for tool path planning is to minimize the machining time. Thus for a given pocket shape (defined by the set *S* in the x-y plane) we want to find the tool path such that this exact shape is machined and the tool path is "optimal".

Held (1991) is a good reference on many mathematical aspects of pocket machining, including the generation of tool paths. Dragomatz and Mann (1997) provides a bibliography on milling path generation literature.

Bieterman and Sandstrom (2003) uses the solution of Laplace's equation defined on the pocket region. The level sets of the principal eigenfunction define a smooth low-curvature spiral path in a pocket interior to one that conforms to the pocket boundary. Their parameterization (by the winding angle) limits the applicability of the method to "nearly convex" shapes, as any ray from the center may only intersect the pocket region boundary once. The spiral tool path generation method based on solving the partial differential equation has difficulty in controlling the distance between two level-set curves. In order to

smooth out the sharp corner of tool path, Pamali (2004) used the clothoid as the transition near the corner of the spiral tool path.

Chuang et al. (2007) generate tool paths based on the 2D Laplace parameterization of pocket contours and the redistribution of the original Laplace isoparametrics. The advantage of this approach is applicability for arbitrary pockets with or without interior islands.

Sun et al. (2006) and Xu et al. (2012) maps the pocket shape onto the unit disk by means of mesh/conformal mapping. On this disk, a guide spiral is constructed and this spiral is then mapped back onto the original pocket shape.

Figure 3 shows a quadrangular pocket (approximately 14×15 cm in size) and tool paths by three different methods. The used tool has diameter 12.7mm and the maximum width of cut is 11 mm.

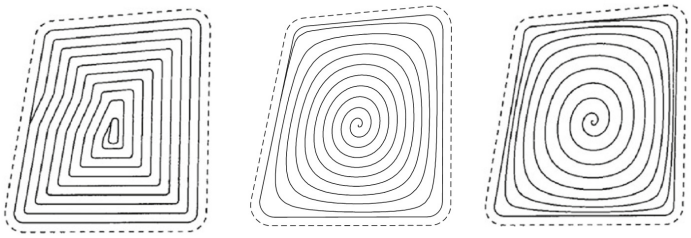

Figure 3. Tool paths for a quadrangular pocket (a) conventional path (b) spiral tool path (Xu et al., 2012) (c) curvilinear path (Bieterman and Sandstrom, 2003)

According to Bieterman and Sandstrom (2003), such spiral tool paths can save around 30% machining time compared to the conventional tool path of Figure 3a. Yao (2006) and Yao and Joneja (2007) utilized generalized spiral curves centered at line segments or curve segments of the medial axis of the pocket for tool path generation.

The method of Held et al. (2009) generates the tool path by interpolating growing disks placed on the medial axis of the pocket and works for arbitrary simply-connected 2D shapes bounded by straight-line segments and circular arcs. The path starts inside the pocket (from a user-specified starting point) and spirals out to the pocket boundary, complying with a user-specified maximum cutting width.

Recently, level set methods (Sethian, 1996) have become popular. These methods are numerical techniques for computing propagating fronts by solving an initial value problem of a partial differential equation. Zhuang et al. (2010) presents a level set approach of tool path generation. The pocket boundary is first embedded into the level set function. To avoid high curvature corners the tool paths are realized by the propagation of the pocket boundary by using a curvature-dependent term.

In this paper, we describe a novel idea for path generation, based on making a correspondence between the state-space trajectories of an oscillator and a two-dimensional path. We describe this idea in detail.

A fast milling simulator based on composite adaptively sampled distance fields has been recently developed at Mitsubishi Electric Research Laboratories. Combining the oscillator-based path planner, the milling simulator and an optimizer, tool paths that are superior to those generated by the classical approaches can be produced.

2. Oscillator-based path planning

Our idea is to find a function $f(x, y)$ that is positive over the given pocket shape *S* (we utilize R-functions for this purpose) and consider this function as the total "energy" of a one-degree-of-freedom oscillator. We make the correspondence between the position x and velocity $\dot{x}$ of the oscillator and the spatial coordinates (x, y). If the oscillator is conservative, the trajectories are (in general) closed curves corresponding to constant total energy and are level sets of $f(x, \dot{x})$. To make a transition between these curves, we introduce damping into the equation of motion of the oscillator.

The correspondence is explained through the following steps.

1. The pocket S and its boundary ∂S can be embedded into a function f(x,y) that is positive over the x-y plane within the pocket shape and zero on the boundary. For example, the pocket S specified is the unit disk ($x^2 + y^2 \leq 1$), and its boundary ∂S is the unit circle $x^2 + y^2 = 1$ as shown in Figure 3a. The boundary is the zero level set of the function $f(x,y) = 1 - (x^2 + y^2)$, i.e. $f(x,y) = 0$ (Figure 3b).

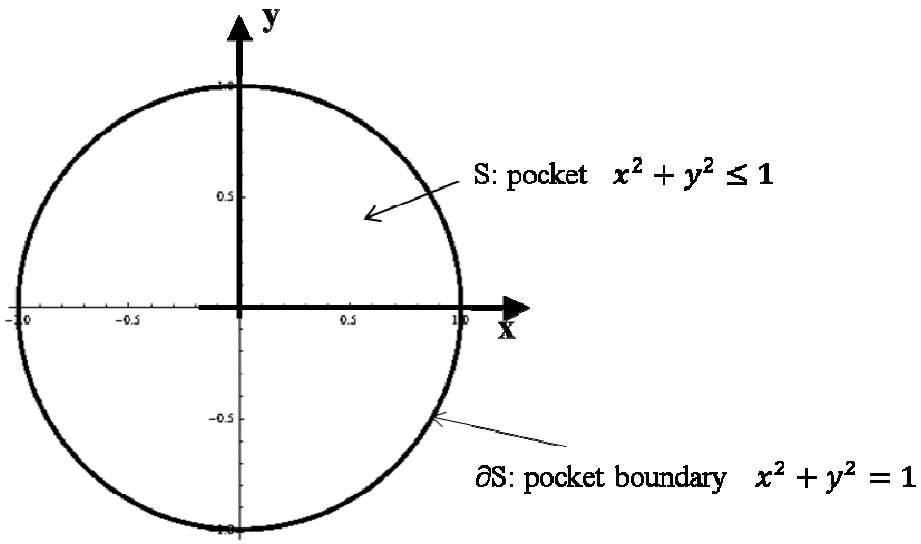

(a) A circular pocket S and its boundary ∂S

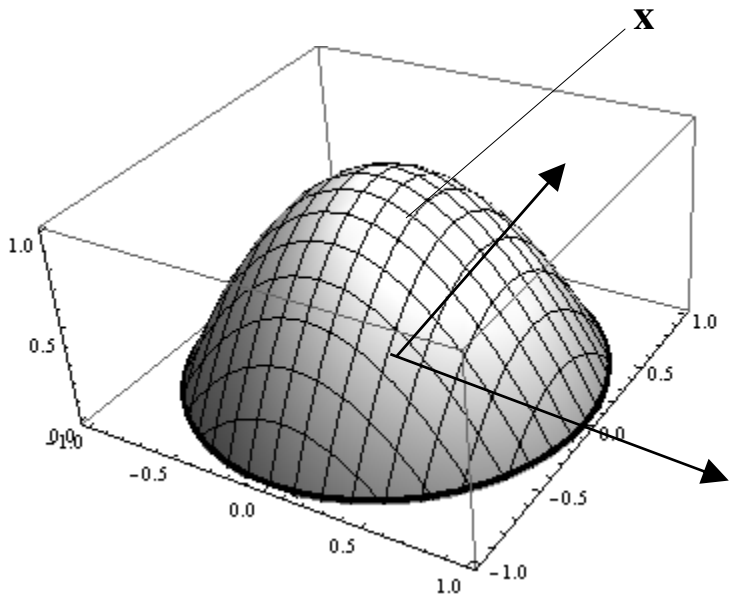

(b)

Figure 3. (a) A pocket and its boundary (b) A positive function over the pocket

2. Consider a 1 degree-of-freedom (DOF) mass-spring (harmonic) oscillator.
The states of this oscillator are position $x(t)$ and velocity $y(t) = \dot{x}(t)$ and t is the independent variable time parametrizing the motion. Closed curves (circles) correspond to the motion of the oscillator with total energy $E(x,\dot{x}) = \frac{1}{2}x^2 + \frac{1}{2}\dot{x}^2 = \text{const.}$
The function

$$f(x,\dot{x}) = 1 - (x^2 + \dot{x}^2) \qquad (1)$$

is positive over the domain $x^2 + y^2 < 1$ and disappears on its boundary, thereby having the "embedding" properties described in 1. The function $f(x,\dot{x})$ is related to the total energy, in that $f(x,\dot{x}) = 1 - 2E(x,\dot{x})$.
3. The equation of motion of the harmonic oscillator can be derived by differentiating the total energy with respect to time as

$$\frac{dE(x,\dot{x})}{dt} = x\dot{x} + \dot{x}\ddot{x} = 0 \Rightarrow \ddot{x} + x = 0. \qquad (2)$$

4. Instead of trying to connect the closed curves corresponding to constant energies of the oscillator obtain a spiral curve, in our method this spiral curve is obtained naturally by adding negative damping into the system (analogous to adding an energy injector to the oscillator, see Figure 4a), resulting in the equation of motion

$$\ddot{x} - 2\xi\dot{x} + x = 0. \qquad (3)$$

The solution of this equation (starting from a point very close to the origin) is a curve (logarithmic spiral) spiraling outward from the origin as shown on the energy surface on the $(x,\dot{x})$ plane in Figure 4b.

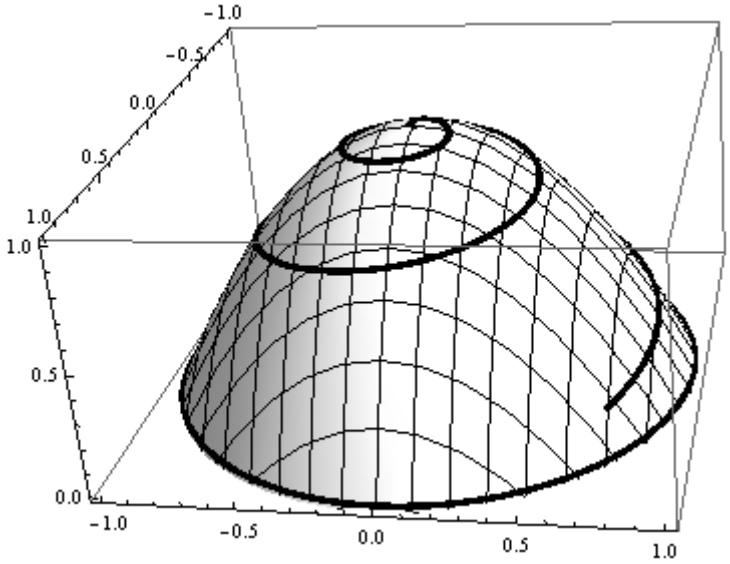

(a) Trajectory on the positive energy function

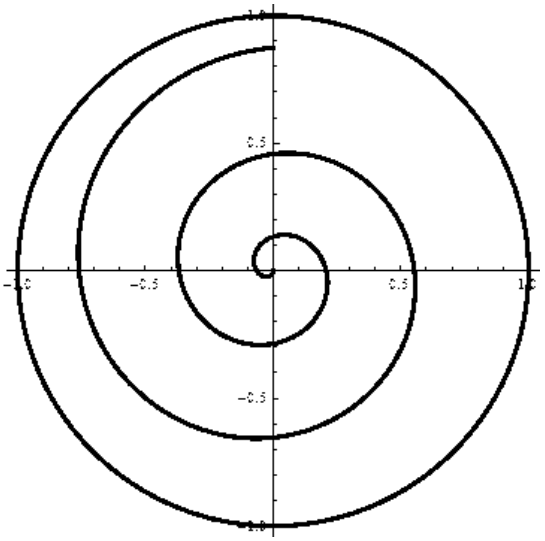

(b) Trajectory in x-x' phase space

Figure 4. (a) Spiral curve over the energy function (b) spiral curve in phase space.

5. To generalize from the example, we construct a function f($\mathbf{x}, \mathbf{y}$) that is positive over the given pocket shape S and zero at the boundary (we use R-functions for this purpose, see next Section) and consider this function as the "total energy" of a one-degree-of-freedom oscillator. The original spatial coordinates $(\mathbf{x},\mathbf{y})$ now correspond to position $\mathbf{x}$ and velocity $\dot{\mathbf{x}}$ of the oscillator. The motion of the oscillator is fully characterized by a trajectory in the $(\mathbf{x}, \dot{\mathbf{x}})$ plane. If the oscillator is conservative, the trajectories are (in general) closed curves corresponding to constant total energy and are level sets of $\mathbf{f}(\mathbf{x}(\mathbf{t}), \dot{\mathbf{x}}(\mathbf{t}))$, i.e.

$$\mathbf{f}(\mathbf{x}(\mathbf{t}), \dot{\mathbf{x}}(\mathbf{t})) = \mathbf{const.} \qquad (4)$$

The equation of motion of the oscillator is found by differentiating eq. (4) with respect to time

$$\frac{\partial f(x(t),\dot{x}(t))}{\partial x(t)}\dot{x}(t) + \frac{\partial f(x(t),\dot{x}(t))}{\partial \dot{x}(t)}\ddot{x}(t) = 0 \qquad (5)$$

To make a transition between the closed curves of this conservative system we introduce a negative damping into the equation of motion (5)

$$\frac{\partial f(x(t),\dot{x}(t))}{\partial x(t)}\dot{x}(t) + \frac{\partial f(x(t),\dot{x}(t))}{\partial \dot{x}(t)}(\ddot{x}(t) - 2\xi\dot{x}) = 0 \qquad (6)$$

The damping coefficient will also serve as a parameter for the optimization problem.

3. A class of functions positive over a domain: R-functions

One possibility for finding functions that are positive over the desired domain is to use the so-called R-functions.

Rvachev (1982) developed the theory of R-functions—real-valued functions that behave as continuous analogs of logical Boolean functions.

More precisely, a real-valued function $f(x_1,x_2, \ldots ,x_n)$ is called an R-function if its sign is completely determined by the signs of its arguments x_i. If the sign of a function is considered to be a logical property, negative values of a function can be considered to correspond with logical FALSE, and positive values can be considered to correspond with logical TRUE. In other words, an R-function f works as a Boolean switching function, changing its sign only when its arguments change their signs; it can be regarded as “on” or “off” (or “true” or “false”) depending on the values of the input variables. For example, the function xyz can be negative only when the number of its negative arguments is odd. As another example, $\min(x_1, x_2)$ is an R-function whose companion Boolean function is logical “and” (Λ) (logical conjunction), and $\max(x_1, x_2)$ is an R-function whose companion Boolean function is logical “or” (V) (logical disjunction). This is seen in that function $\min(x_1, x_2)$ takes on positive values only when x_1 AND x_2 are positive; similarly function $\max(x_1, x_2)$ takes on positive values when x_1 OR x_2 are positive.

A large number of R-functions are known and catalogued (see, e.g., Rvachev (1982) and Shapiro and Tsukanov (1999)), and have been assigned unique names such as R_α, R_0^m, R_p, and the like depending on their nature and properties. To illustrate, the R-function R_α is defined by:

$$R_\alpha: f = \frac{1}{1+\alpha}\left(x_1 + x_2 \pm \sqrt{x_2^2 + x_2^2 - 2\alpha x_1^2 x_2^2}\right) \qquad (6)$$

where $\alpha(x_1,x_2)$ is an arbitrary function such that $-1<\alpha(x_1,x_2)\leqq 1$. The precise value of α may or may not matter, and often it can be set to a constant. For example, setting α=1 yields the functions min and max respectively, but setting α=0 results in functions V_0 and Λ_0 that are analytic everywhere (i.e., can be represented by a convergent Taylor series), except when $x_1=x_2=0$.

As another example, consider the R-function R_0^m:

$$R_0^m: f=(x_1+x_2\pm\sqrt{x_1^2+x_2^2})(x_1^2+x_2^2)^{m/2} \qquad (7)$$

where m is any even positive integer. This function is also analytic everywhere except at the origin $x_1=x_2=0$, where it is m times differentiable.

Similarly, for the R-function R_p:

$$R_p: f = x_1 + x_2 \pm (x_1^p + x_2^p)^{1/p} \quad (8)$$

the function is analytic everywhere for any even positive integer p.

In the foregoing expressions, choosing the (+/–) sign of arguments determines the type of R-function: (+) corresponds to R-disjunction (Boolean "or"), and (–) gives the corresponding R-conjunction (Boolean "and") of the real-valued arguments x and y.

Similarly to Boolean functions, R-functions are closed under composition, which means that a combination of several R-functions is another R-function which corresponds to a more complex logical expression. Thus, just as any logical function can be written using only three operations (logical negation or NOT), V (logical disjunction or OR), and Λ (logical conjunction or AND), three corresponding R-functions can be combined into a corresponding R-function. Expressed another way, for every formal logical sentence (i.e., for every Boolean function), one may construct a corresponding R-function using R-conjunction, R-disjunction, and R-negation, whose sign is determined by the truth table of the logical sentence. For nonzero arguments, the negation operation is usually accomplished by changing the sign of the R-function. The logical disjunction Λ and conjunction V operations can respectively be accomplished in the usual case by performing intersection and union operations. Depending on the particular form of the R-conjunction, R-disjunction, and R-negation chosen to construct the corresponding R-function (i.e., depending on the "family" R_0^m, R_p, etc. from which the R-functions are chosen), a rich variety of differential properties may be obtained.

The geometric model is then represented implicitly by functions, called for brevity "implicit functions". Defined generally, an implicit equation relates two or more variables such that for any value of one variable, there are values of the others which make the equation true; thus, the one variable is defined as a function of the others. In the context of the invention, an implicit function is a function $f(x_1,x_2, \ldots ,x_n)=y$ that takes on zero values at desired locations in space; in other words, the zero set of the function implies the geometry of the defined set of points making up the geometric model.

The implicit functions therefore define the geometric model (or portions thereof) by having points within the model and/or its boundary take a zero value and points outside the model take other discrete values. R-functions can be used to construct implicit functions.

An example using R-functions for milling path generation using our idea is shown in Figure 5.

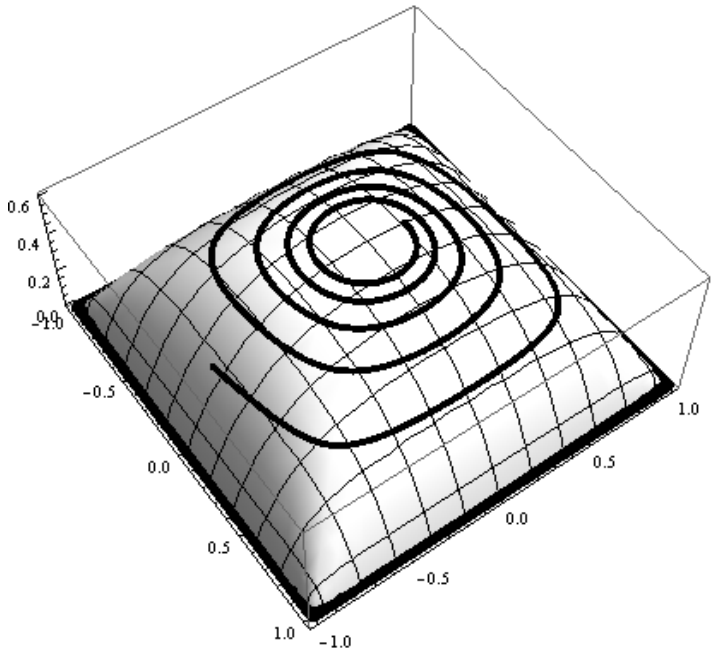

(a) Oscillator-based trajectory on a square domain

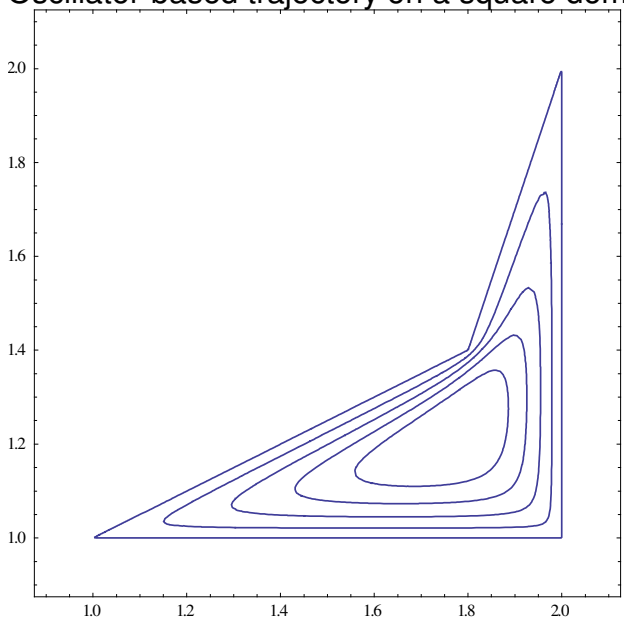

(b) Level curves for a non-convex domain

Figure 5 (a) Milling path in a square pocket (b) Level curves for a non-convex pocket shape.

4. Distance Fields Based NC Milling Simulation

The cut shape is found by translating (sweeping) the shape of the cutting tool over its trajectory (we assume that the cutting process is planar and unencumbered by dynamic effects, i.e. the milling tool is rigid and has uniform cross section). To formalize this, we utilize the so-called Minkowski sum. The Minkowski sum of two sets of position vectors A and B is formed as $A \oplus B = \{a + b | a \epsilon A, b \epsilon B\}$, where each vector in *A* and each vector in *B*

are added. The tool (characterized by the set T describing its shape) moving along the path $P = \{(x(t), y(t)), t \in [0,1]\}$ cuts the pocket shape *S*, which is defined as $S = P \oplus T$.

We have proposed a new approach to NC milling simulation that can rapidly generate a highly accurate representation of the milled workpiece. In this new representation each surface is implicitly represented by the signed Euclidean distance field

$$d_S(P) = \begin{cases} \inf_{\forall q \in \partial S} \|P - q\|_2 & P \in S \\ -\inf_{\forall q \in \partial S} \|P - q\|_2 & P \notin S \end{cases} \qquad (9)$$

This function yields the minimum Euclidean distance from a point ***P*** to the closest in the boundary of the set ∂S. An octree bounding volume hierarchy is used to obtain spatial localization of geometric operations.

4.1 Distance fields of 5-axis motions

In this section, we develop a mathematical formulation for computing the swept volumes of general surfaces of revolution. The Cutter Workpiece Engagement (CWE) surface is the instantaneous intersection between the tool at final position and in-process workpiece as given in Figure 6. Sweeping an arbitrary set of points *S* along a motion *M* in a space is usually formulated as an infinite union operation expressed formally as,

$$sweep(S, M) = \bigcup_{q \in M} S^q \qquad (10)$$

where S^q denotes the set *S* positioned according to a configuration q of motion *M(t)*, within a normalized interval. *M(t)* is a one parameter family of rigid body transformations in E^3. The distance from a point ***P*** in the space to the boundary of swept volume is defined in the world coordinate frame;

$$d_S(P, sweep(S, M(t))) = \inf_{q \in \partial sweep(S, M(t))} \|P - q\|_2 \quad (11)$$

Finding the distance field of a swept volume requires computing the envelopes of the swept volume. This process is difficult for general 5-axis motions. Instead the computation of distance field is handled by an inverted trajectory approach where the problem is solved in tool coordinate frame instead of world coordinate frame.

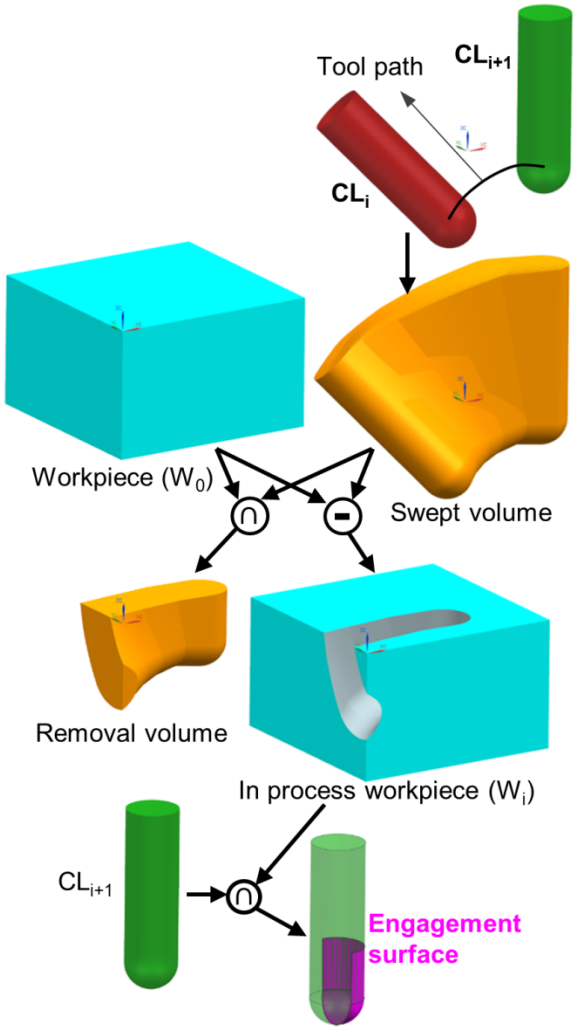

Figure 6. Calculation of the CWE surface using Boolean operations

When the test point ***P*** is viewed in tool coordinate frame, it moves along an inverted trajectory, $\hat{T}_P$ which is defined according to the inverse of the motion *M(t)*. In this tool coordinate frame, the distance field is now defined by,

$$dist(S,\hat{T}_P) = \min_{y\in\partial S, z\in\hat{T}_P} \|y-z\|_2 \qquad (12)$$

In the 3-axis milling case, the tool axis is always constant in one direction, translates in space and only rotates around its own axis, however, in 5-axis milling case, addition of two rotational axes allow to machine variety of different workpieces and motions. Compared to 3-axis machining, the inverted trajectory has a more complex geometry because of the rotational effects as seen in Figure 7. Besides three translational movements, the tool can also be rotated around two axes. The minimum distance between the inverted trajectory and tool can be computed by using numerical search methods. Direct analytical solution of the minimum distance function is rather difficult; hence it is cast as a one-dimensional minimization problem. It is solved by employing an iterative numerical method which combines the golden section search and inverse quadratic interpolation.

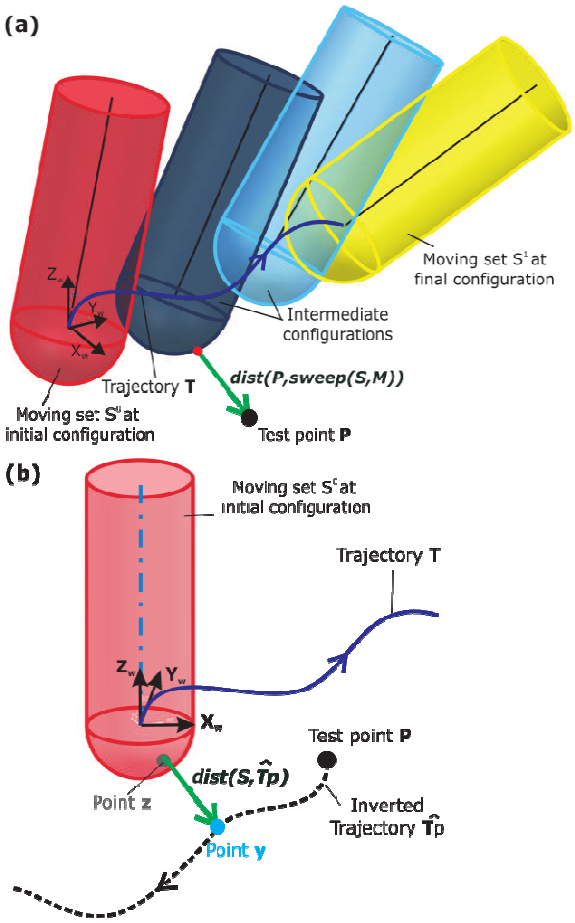

Figure 7. 5-axis motion and inverted trajectory

Figures 8 and 9 show the proposed algorithms to compute milling paths as well as to optimize these paths with respect to various user-chosen metrics.
Concrete examples will be discussed in the full-length paper (this is subject to approval of Mitsubishi Electric).

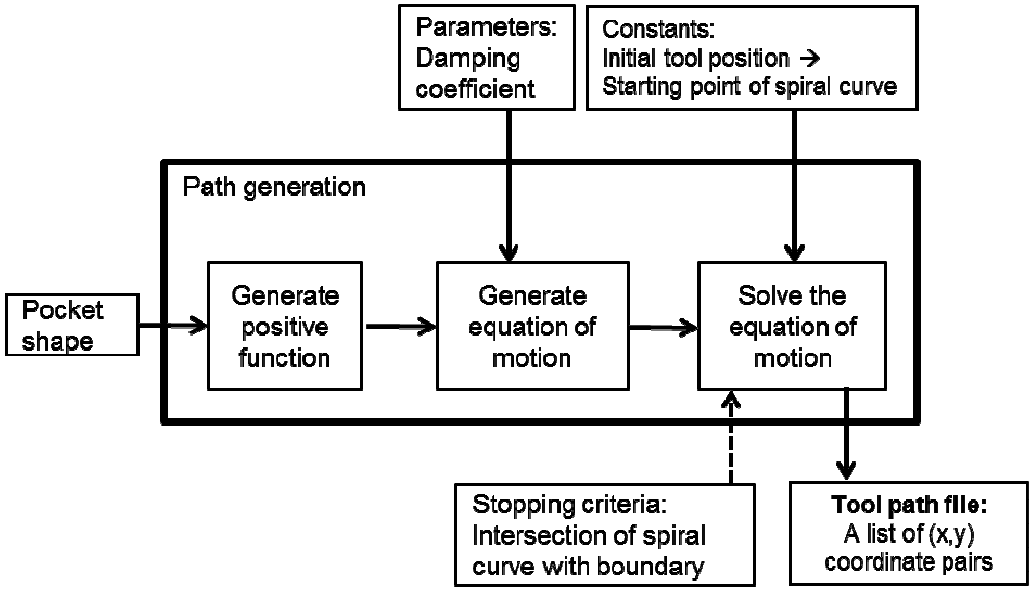

Figure 8. The flow diagram of a method for path generation

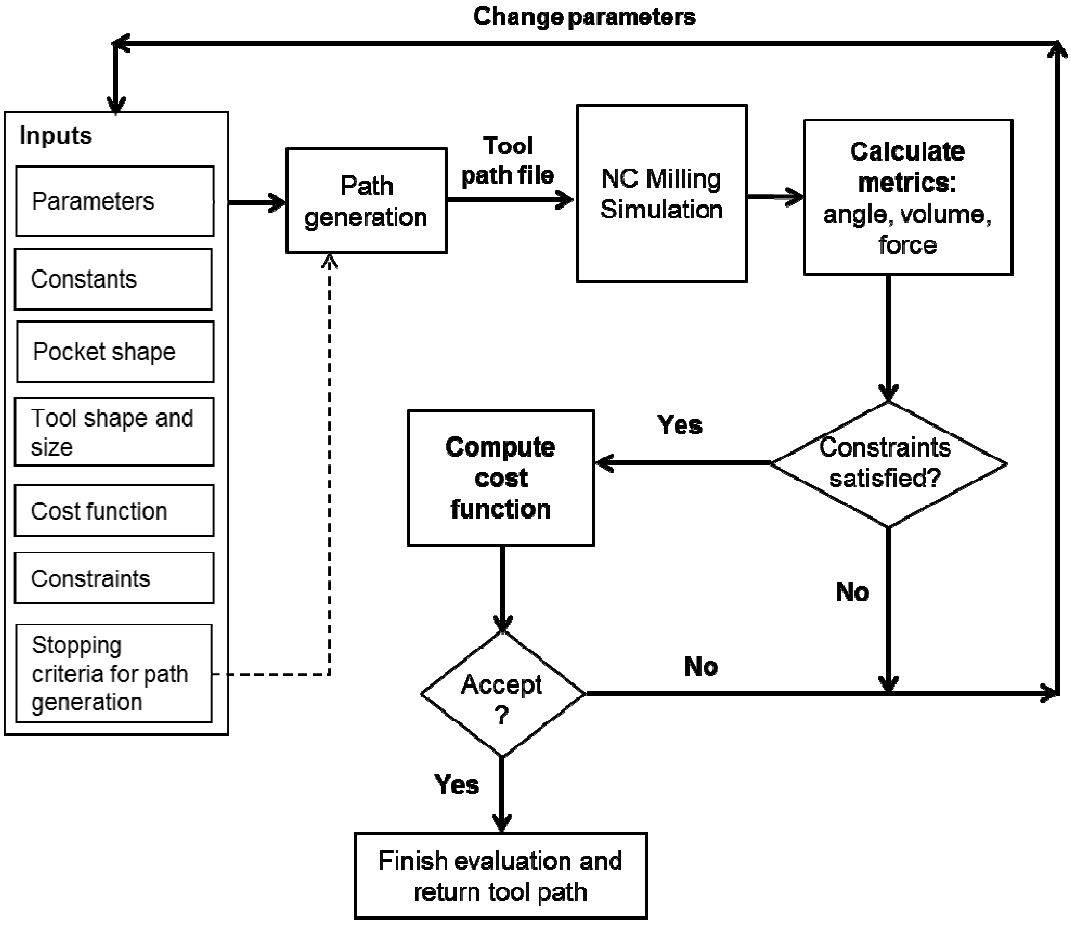

Figure 9. The flow diagram of a method for determining the tool path for NC pocket milling

References

1. Bieterman, Michael B., and Donald R. Sandstrom. "A curvilinear tool-path method for pocket machining." *Journal of manufacturing science and engineering* 125, no. 4 (2003): 709-715.

2. Wang, Hongcheng, Peter Jang, and James A. Stori. "A metric-based approach to two-dimensional (2D) tool-path optimization for high-speed machining." TRANSACTIONS-AMERICAN SOCIETY OF MECHANICAL ENGINEERS JOURNAL OF MANUFACTURING SCIENCE AND ENGINEERING 127.1 (2005): 33.

3. Held, Martin. *On the computational geometry of pocket machining*. Vol. 500. Springer, 1991.

4. Chuang, Jui-Jen, and Daniel CH Yang. "A Laplace-based spiral contouring method for general pocket machining." *The International Journal of Advanced Manufacturing Technology* 34, no. 7-8 (2007): 714-723.

5. Xu, Jinting, Yuwen Sun, and Xiangkui Zhang. "A mapping-based spiral cutting strategy for pocket machining." *The International Journal of Advanced Manufacturing Technology* (2012): 1-12.

6. Yao, Zhiyang. "A novel cutter path planning approach to high speed machining." *Computer-Aided Design and Applications* 3, no. 1-4 (2006): 241-248.

7. Yao, Zhiyang, and Ajay Joneja. "Path generation for high speed machining using spiral curves." *Computer-Aided Design & Applications* 4 (2007): 191-198.

8. Held, Martin, and Christian Spielberger. "A smooth spiral tool path for high speed machining of 2D pockets." *Computer-Aided Design* 41, no. 7 (2009): 539-550.

9. Makhanov, Stanislav S. "Adaptable geometric patterns for five-axis machining: a survey." The International Journal of Advanced Manufacturing Technology 47.9-12 (2010): 1167-1208.

10. Zhuang, Chungang, Zhenhua Xiong, and Han Ding. "High speed machining tool path generation for pockets using level sets." *International Journal of Production Research* 48, no. 19 (2010): 5749-5766.

11. Sethian, James A. "A fast marching level set method for monotonically advancing fronts." *Proceedings of the National Academy of Sciences* 93, no. 4 (1996): 1591-1595.

12. Sethian, J.A., 1999.Level set methods and fast marching methods. Cambridge, UK: Cambridge
13. University Press.

14. Osher, S. and Fedkiw, R., 2003.Level set method and dynamic implicit surface. New York: Springer–Verlag

15. Sun, Yu-Wen, Dong-Ming Guo, and Zhen-Yuan Jia. "Spiral cutting operation strategy for machining of sculptured surfaces by conformal map approach." *Journal of materials processing technology* 180, no. 1 (2006): 74-82.

16. Kim, Taejung, and Sanjay E. Sarma. "Toolpath generation along directions of maximum kinematic performance; a first cut at machine-optimal paths." Computer-Aided Design 34.6 (2002): 453-468.

17. Dragomatz, D., and S. Mann. "A classified bibliography of literature on NC milling path generation." *Computer-Aided Design* 29, no. 3 (1997): 239-247.

18. Arkin, Esther M., Sándor P. Fekete, and Joseph SB Mitchell. "Approximation algorithms for lawn mowing and milling." Computational Geometry 17.1 (2000): 25-50.

19. Balestrino, A., et al. "Stability analysis of dynamical systems via R-functions." Proc. of the IEEE European Control Conference, Budapest (Hungary). 2009.

20. Pamali, Abhinand P. "Using clothoidal spirals to generate smooth tool paths for high speed machining." (2004).

21. D. Biermann, T. Surmann, P. Kersting Oscillator-based approach for modeling process dynamics in NC milling with position- and time-dependent modal parameters

22. V. L. Rvachev, *Theory of R-functions and Some Applications*, Naukova Dumka, 1982

23. V. Shapiro and I. Tsukanov, Implicit functions with guaranteed differential properties, *Fifth ACM Symposium on Solid Modeling and Applications*, Ann Arbor, Mich., 1999